ACS APPLIED MATERIALS & INTERFACES

Research Article

www.acsami.org

Copper Impurity Effects on $LiNi_{1/3}Mn_{1/3}Co_{1/3}O_2$ Cathode Material

Qina Sa, Joseph A. Heelan, Yuan Lu, Diran Apelian, and Yan Wang*

Department of Mechanical Engineering, Worcester Polytechnic Institute, 100 Institute Road, Worcester, Massachusetts 01609, United States

ABSTRACT: The crystal structure and electrochemical properties of $LiNi_{1/3}Mn_{1/3}Co_{1/3}O_2$ (NMC) synthesized from a lithium ion battery recovery stream have been studied previously. In this report, we study the Cu impurity effects on NMC in detail. The difference in crystal structures and electrochemical properties were examined for pure and copper impurity included products. Scanning electron microscopy figures show that the precursor particles of NMC are slightly bigger than that of NMC with copper impurity. After undergoing 150 cycles at 2C, X-ray diffraction refinements results show that the lattice parameters for impurity containing NMC and pure NMC change to different extents. Furthermore, due to the minor change of lattice parameters, copper-containing NMC offers a more stable capacity retention compared to pure NMC.

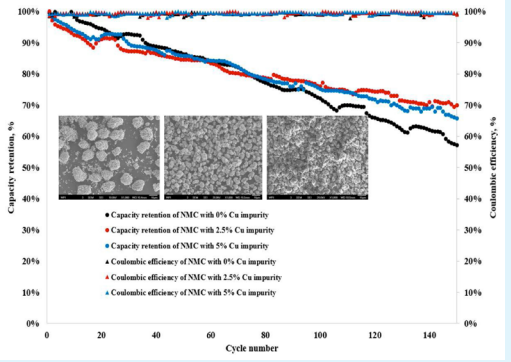

KEYWORDS: *lithium ion battery recovery, $LiNi_{1/3}Mn_{1/3}Co_{1/3}O_2$, copper impurity, $Ni_{1/3}Mn_{1/3}Co_{1/3}(OH)_2$, particle size, electrochemistry*

1. INTRODUCTION

Worldwide demand of lithium ion batteries indicates that the amount of lithium ion battery waste will increase annually and could become a potential issue for the environment.[1] Motivated by this fact, researchers have been working on developing various lithium ion battery recycling processes.[2−6] A low-cost and high-efficiency lithium ion battery recovery process has been proposed and introduced in detail,[7,8] in which the recovery efficiencies of nickel, cobalt, and manganese metal values are over 90%. A solution containing leached cathode powders from a recycled battery stream was utilized to synthesize NMC.[9] Because the cathode material was synthesized from the leaching solution of a lithium ion battery recovery stream, possible impurity elements such as copper, aluminum and iron do exist. The source of the copper is the copper current collector of the anode, whereas the source of the aluminum is the copper current collector cathode. Iron comes from the battery's steel case, $LiFePO_4$, or both. Due to the very low solubility constant, Al^{3+} and Fe^{3+} are easily removed by controlling the pH of the solution. However, Cu^{2+} is difficult to completely eliminate due to its higher solubility constant. Ni^{2+}, Mn^{2+}, and Co^{2+} could also precipitate when the pH is high enough, which will lower the recovery efficiency of these three valuable metal elements. Therefore, it is critical to understand how the presence of copper might affect the crystal structure and electrochemical performance of NMC.

It has been reported that element doping is one efficient way to improve the electrochemical properties of cathode materials.[10−12] But there is no report of copper doping of NMC. The objective of this research work was to examine how copper impurity would affect the electrochemical properties of cathode. After performing experiments, we found that the addition of copper lowers the specific rate performance but improves the cycle life of NMC. At the beginning of cycle life test, the capacity of pure NMC is higher than that of NMC with copper. However, the capacity retention of NMC with copper is better than that of pure NMC over time and will have a better overall capacity after 150 cycles are completed.

In this work, pure NMC and NMC with controlled copper amount were synthesized via coprecipitation process[13−16] and solid-state synthesis process.[17−19] Once the precursors and cathodes were obtained, SEM, XRD, and electrochemical tests were conducted to examine how the presence of copper affected the materials' properties and performance using pure NMC as a baseline comparison. It was found that copper element does affect the particle size of coprecipitated precursors. The particle size of copper included precursor is smaller than that of pure NMC precursor. Also, the electrochemical test results of cathode materials show that the NMC with copper impurity performs lower specific rate capacities but reveals better capacity retention during cycling test.

2. EXPERIMENTAL SECTION

2.1. Synthesis of NMC Cathode Materials. Before synthesizing NMC cathode materials with and without copper impurity, $Ni_{1/3}Co_{1/3}Co_{1/3}(OH)_2$ precursors with and without copper impurity were synthesized first. The synthesis details are as follows. The hydroxides were obtained via a coprecipitation process involving NaOH and $NH_3{\cdot}H_2O$ solutions. In the experiment, 1000 mL of 1 M $NH_3{\cdot}H_2O$ was first put into the reactor and heated up to 60 °C. Then,

Received: May 22, 2015
Accepted: August 31, 2015
Published: September 1, 2015

DOI: 10.1021/acsami.5b04426
ACS Appl. Mater. Interfaces 2015, 7, 20585−20590

5 M $NH_3{\cdot}H_2O$ and 2 M MSO_4 (M: Co, Mn, Ni) solutions were pumped into the reactor at adding rates of 10 and 30 mL/h, respectively. Next, 5 M NaOH was automatically added into the reactor throughout the reaction by a pH controlled peristaltic pump to stabilize the reaction at a desired pH. The feeding time of MSO_4 and $NH_3{\cdot}H_2O$ was 10 h. After MSO_4 addition, the material was stirred in solution for an additional 24 h. An overhead stirrer was utilized, and the stirring speed was 750 rpm. The synthesized precursors were filtered and washed until the pH of filtering solution reduced to 7, then it was dried in an oven at 110 °C overnight. When synthesizing the precursor with copper impurity, we added the desired amounts of $CuSO_4$ to the MSO_4 solution prior to the coprecipitation process and the experiment was repeated.

To synthesize the $LiNi_{1/3}Mn_{1/3}Co_{1/3}O_2$ cathodes, $Ni_{1/3}Co_{1/3}Co_{1/3}(OH)_2$ precursors was thoroughly mixed with Li_2CO_3 by mortar and pestle. The mixture was heated to 900 °C for 12 h. The material was heated in air for 12 h and both the heating rate and cooling rate were 2 °C/min.

2.2. Battery Assembling and Electrochemical Property Test with Synthesized NMC Cathode Materials. The lithium ion battery electrode was prepared from the mixture of 10 wt % polyvinylidene fluorides (PVDF) binder, 10 wt % conductive additive C65, and 80 wt % synthesized $LiNi_{1/3}Mn_{1/3}Co_{1/3}O_2$ cathode materials. The mixed slurry was then cast onto an aluminum foil current collector. The electrode was dried in the oven overnight at 60 °C. After the electrode was completely dried, a piece of $^1/_4$ in. diameter electrode was punched out of the electrode sheet and pressed to a thickness of 50 μm; the loading mass was 5 mg/cm^2. The electrochemical properties were tested by assembling Swagelok cells in an argon gas filled glovebox. The electrolyte was 1 M $LiPF_6$ dissolved in ethylene carbonate, dimethyl carbonate and diethyl carbonate (EC+DMC+DEC, 1:1:1 in volume). Lithium metal served as the anode during the electrochemical test. All tests were conducted at room temperature.

2.3. Characterizations. Inductive Coupled Plasma- optical emission spectrometry (ICP-OES) (PerkinElmer Optical Emission Spectrometer, Optima 8000) was utilized to measure the concentrations of all the metallic elements in solution. X-ray diffraction (XRD) pattern was obtained from diffractometer (PANalytical Empyrean Series 2 X-ray Diffraction System, with chromium Kα radiation, Cr target) by scanning the powder with a 2θ range of 20–120° at a step size of 0.008° and scanning step time 20 s. The operation voltage and current of XRD machine were 30 kV and 55 mA, respectively. HighScore Plus program was utilized to perform Rietveld refinements. The particle size and morphology were observed by scanning electron microscopy (SEM) (JEOL JSM-7000F electron microscope). The electrochemical performance was examined using an Arbin electrochemical tester. The rate capacities for electrochemical testing included C/10, C/5, C/3, C/2, C, 2C and 4C. 2C cycle life tests were performed to examine the capacity retention performance of different cathode materials. The cut off voltage was 4.3 V for charging and 2.7 V for discharging. The 1C rate was calculated as 160 mAh/g. Cyclic voltammetry (CV) scan of 2.5 V to 4.8 V was taken at 0.1 mV for 2 cycles.

3. RESULTS AND DISCUSSION

3.1. ICP-OES Characterization of NMC Materials. Three samples with different amount of copper impurities (0, 2.5, and 5 atom %) were synthesized and compared. The objective was to examine how the copper impurity affects the NMC cathode properties. To confirm copper element is present in the synthesized cathode materials, 0.05 g of each sample was leached using 20 mL of leaching reagent and sent to ICP-OES test. Table 1 is showing the atomic percentages of Ni, Mn, Co, and Cu in the synthesized cathode materials. The ICP-OES results show that the copper element does exist in the resulting product. The atomic percent of copper relative to the other transition metals were 2.3 and 4.6 atom % in the two synthesized samples. These numbers are slightly lower than the expected 2.5 and 5%, but considering errors from the synthesis process and ICP-OES equipment, the resulting data is acceptable. ICP-OES results only provide the information about the existence of copper, whether the copper impurity is locating inside or outside the crystal structure of NMC cathode is still unsure. This will be discussed again in section 3.3 according to the XRD data.

Table 1. Metal Element Atomic Percentages in Different NMC Samples

	Ni (%)	Mn (%)	Co (%)	Cu (%)
NMC prepared with 0 atom % Cu solution	32.80	35.70	31.50	0.00
NMC prepared with 2.5 atom % Cu solution	34.00	31.70	32.00	2.30
NMC prepared with 5 atom % Cu solution	33.40	30.50	31.50	4.60

3.2. Particle Morphologies of Precursors and NMC Cathode with and without Copper Impurity. Figure 1 shows particle size difference of $Ni_{1/3}Mn_{1/3}Co_{1/3}(OH)_2$ with 0, 2.5, and 5 atom % copper impurity and their corresponding cathodes. In the coprecipitation process, the existence of copper affects the particle size of the precursor. Although the synthesis condition is the same, $Ni_{1/3}Mn_{1/3}Co_{1/3}(OH)_2$ with copper impurity shows a relatively smaller particle size which is 5–8 μm, compared to a 10–15 μm particle size in the pure $Ni_{1/3}Mn_{1/3}Co_{1/3}(OH)_2$. The particle size and morphologies remained from precursors to cathodes. The reaction equilibrium of coprecipitation is determined by many factors such as temperature, feeding rates, pH values, and so on. Ni and Co can form $[M(NH_3)_n]^{2+}$, and when Mn is involved, the three together form $[Ni_{1/3}Mn_{1/3}Co_{1/3}(NH_3)_n]^{2+}$.[21] The addition of Cu can make the system even more complicated. The particle growth mechanism of coprecipitation reaction is that $[M(NH_3)_n]^{3+}/M(OH)_2$ (M = Ni, Mn, and Co) reaches equilibrium at certain pH (pH = 10 in this work) by controlling the feeding rates of MSO_4 solution, NaOH, and ammonia–water. Then M^{2+} will be slowly precipitated out from $[M(NH_3)_n]^{3+}$ and convert to $M(OH)_2$, allowing the $M(OH)_2$ nuclei to grow to bigger size particles.[22] When Cu impurity exists in the system, $Cu(OH)_2$ has the lowest solubility value compared to the hydroxide phase of the other three[21] and this will affect the reaction equilibrium of the $[M(NH_3)_n]^{3+}/M(OH)_2$ (M = Ni, Mn, and Co) complex thus preventing the particle growth of Co, Ni, and Mn hydroxides.

3.3. Crystal Structure Analysis of Synthesized NMC Products. Figure 2 shows the refinement patterns of the 6 samples: NMC with 0, 2.5, and 5 atom % Cu before (Figure 2a) and after (Figure 2b) 2C cycling. No impurity peaks related to copper compounds were identified, which indicates copper element does not change the crystal structure of NMC. There are several reports about metal doping of cathode materials, in which they demonstrated that the dopant replaced the transition metals in the crystal structure.[10−12] Because the location of the copper element is very close to nickel, cobalt and manganese in periodic tables, it has similar chemical properties with Ni, Mn, and Co. Therefore, it is highly possible that the copper impurity occupied some of the transition metal sites. However, the exact location of Cu in the crystal structure is still unclear.

DOI: 10.1021/acsami.5b04426
ACS Appl. Mater. Interfaces 2015, 7, 20585–20590

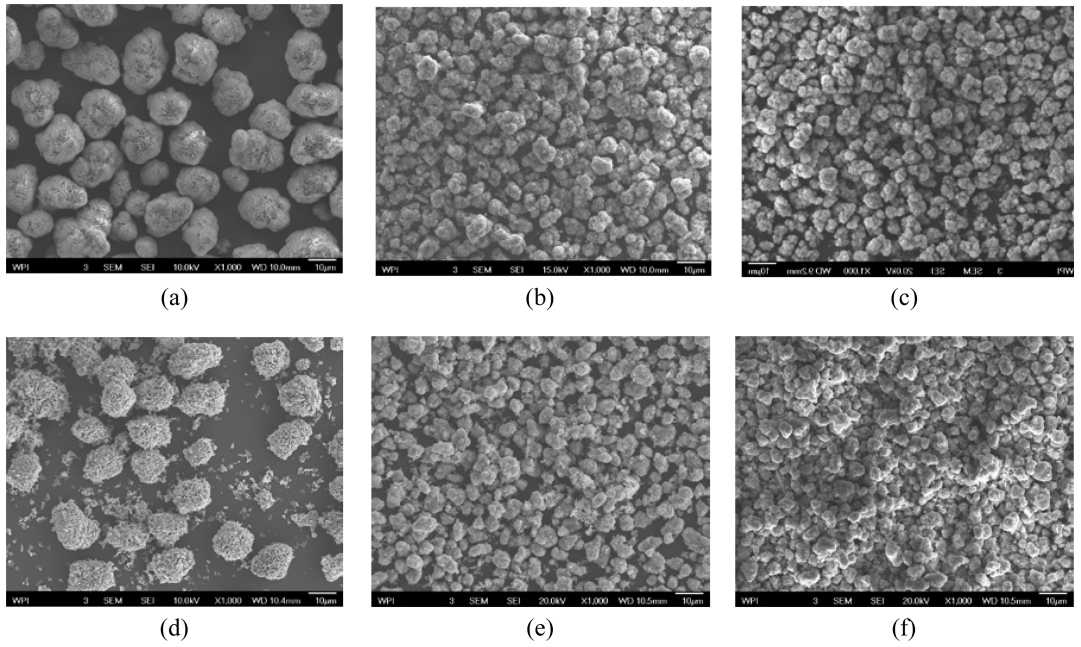

Figure 1. SEM micrographs of precursor and cathodes synthesized with and without copper impurity. (a) $Ni_{1/3}Mn_{1/3}Co_{1/3}(OH)_2$ with 0% Cu, (b) $Ni_{1/3}Mn_{1/3}Co_{1/3}(OH)_2$ with 2.5% Cu, and (c) $Ni_{1/3}Mn_{1/3}Co_{1/3}(OH)_2$ with 5% Cu, (d) NMC with 0% Cu, (e) NMC with 2.5% Cu, (f) NMC with 5% Cu.

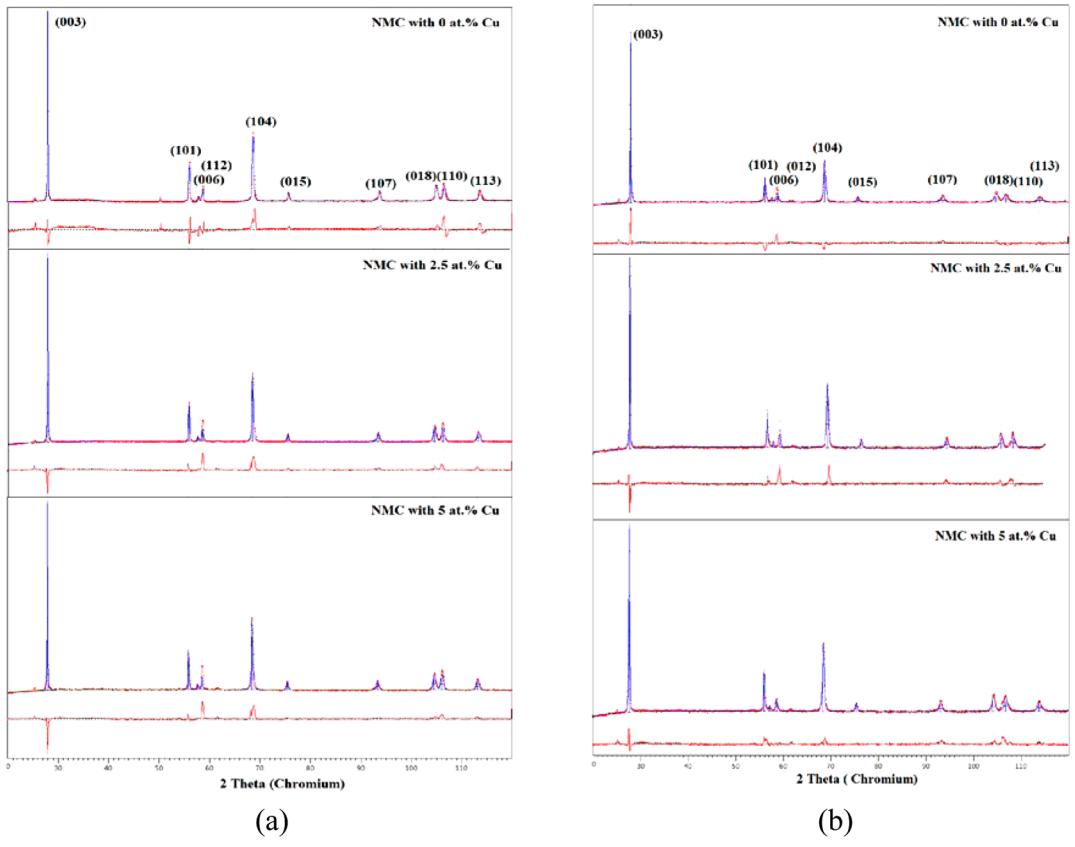

Figure 2. (a) XRD refinement patterns of NMC with different amount of copper before cycling test, (b) XRD refinement patterns of NMC with different amount of copper after cycling test.

Table 2 shows the XRD refinement results. All crystal structures have a *c*/*a* ratio greater than 4.97. The I(003)/I(104) is higher than 1.7. The pattern shows that clear splitting of the (006) and (012) peaks indicating the appropriate layered structure had formed. For pure NMC, parameter *c* increases 0.6% after cycling, and *c* values of NMC with 2.5 and 5 atom % Cu increases 0.1 and 0.4%, respectively. The lattice parameter c represents the distance of the layered structure, and this layered

DOI: 10.1021/acsami.5b04426
ACS Appl. Mater. Interfaces 2015, 7, 20585−20590

Table 2. XRD Refinement Results of Synthesized Cathode Materials

	before cycling test				after cycling test				
	a (Å)	*c* (Å)	*c*/*a*	Rwp	*a* (Å)	*c* (Å)	*c*/*a*	Rwp	*c* value variation (%)
NMC with 0 atom % Cu	2.857	14.228	4.980	9.240	2.849	14.315	5.024	8.100	0.60
NMC with 2.5 atom % Cu	2.866	14.259	4.975	8.520	2.852	14.271	5.003	8.440	0.10
NMC with 5 atom % Cu	2.865	14.268	4.981	8.290	2.850	14.333	5.029	6.430	0.40

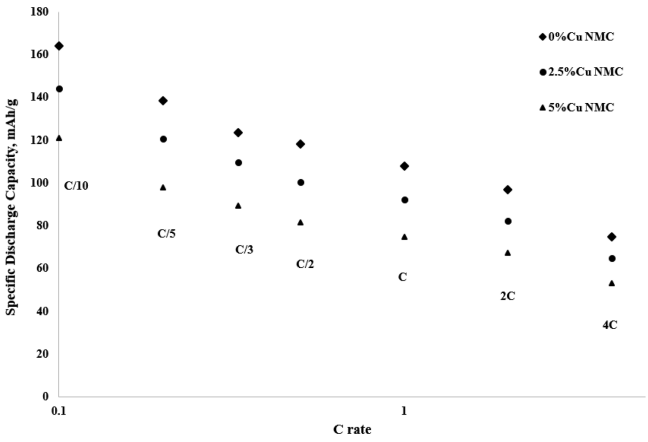

Figure 3. Specific rate capacity test results of NMC with 0, 2.5, and 5 atom % Cu.

structure relates to the amount of lithium ions between the two layers of MO_2^-.[20] The absence of lithium ions leads to the two negative charged oxides layers losing the bonding connection, as two layers with negative charges will repel each other. During the delithiation−lithiation process between 2.7 to 4.3 V, transition metals, such as Co and Ni, are oxidized to M^{4+}. Mn^{4+} is electrochemically inactive but contributing to the layered structure stability.[23] So the question would be, what is the activity of Cu in the crystal structure? If a small amount of electrochemical inactive Mn^{4+} sites were occupied by Cu^{2+} or Cu^+, Cu ions can be oxidized to Cu^{2+} or reduced to Cu^+. This causes the Cu element to be active for electrochemical reactions and contributes to capacity retention improvement. Therefore, in this case, as the capacity is fading in pure NMC, the Cu^{2+}/Cu^+ ions in NMC with Cu impurity can still be active for reacting with Li ions. So after cycling, fewer lithium ions remained in the layer structures of pure NMC compared to Cu contained-NMC, causing parameter *c* to increase in pure NMC and the capacity retention to drop. The CV scan results provide more information for the discussion of Cu activity as can be seen in the following section.

3.4. Electrochemical Test Results. Rate capacity test results are shown in Figure 3. At C/10, pure NMC has a discharge capacity of 161 mAh/g, and NMC with Cu impurities shows lower specific discharge capacities. As the amount of Cu increases, the discharge capacities of NMC decreases. This decreasing pattern of discharge capacities is also apparent at other C rates. These results indicate that Cu element as an impurity to NMC cathode material, does not change the crystal structure significantly from one phase to another, because the XRD patterns of three samples look similar, but it does result in some defects in the layered structure. So, the layer structures of NMC with impurity will not be as good as that of pure NMC, and the specific rate performance of NMCs with impurity is lower. The first cycle charge and discharge curves are shown in Figure 4. The first cycle efficiency for pure NMC cathode, 2.5 atom % NMC cathode, and 5 atom % NMC cathode are 87, 84, and 82% respectively.

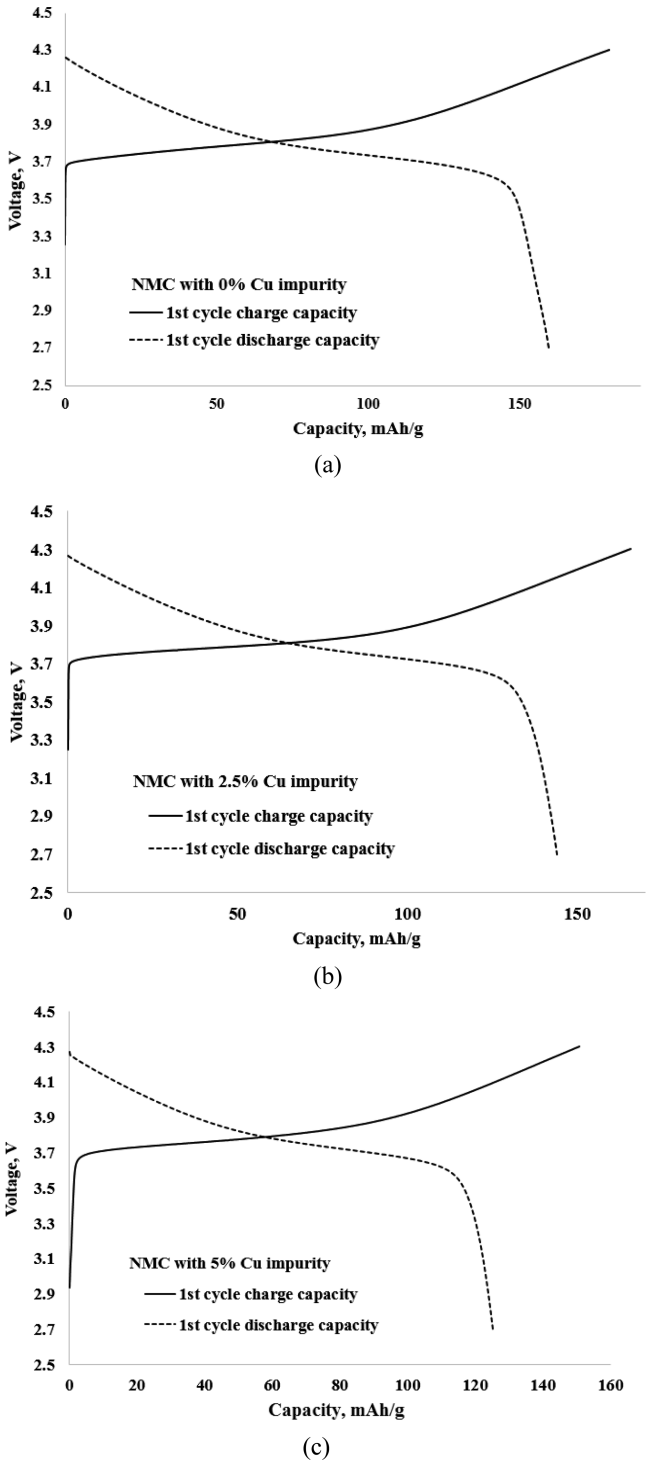

Figure 4. First cycle charge and discharge curves of NMC with different amount copper impurity.

DOI: 10.1021/acsami.5b04426
ACS Appl. Mater. Interfaces 2015, 7, 20585−20590

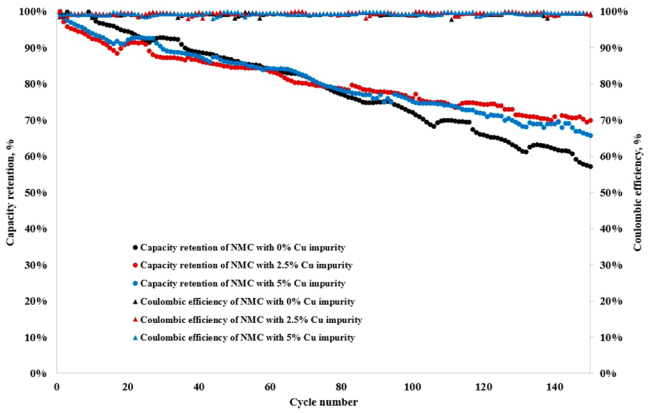

Figure 5. Capacity retention results of NMC with 0, 2.5, and 5 atom % copper (2C, 2.7−4.3 V).

Capacity retention tests were performed by cycling the cells at 2C (Figure 5). At the beginning, pure NMC offers better capacity performance. It achieves a discharge capacity of 100 mAh/g discharge capacity at 2C. However, the overall capacity retention of NMC with Cu impurities is better than that of the pure product. In addition, the capacity retention of NMC with 2.5% Cu is slightly better than that with 5% Cu. These results agree well with the previously discussed parameter *c* change conclusion. The capacity retention of pure NMC drops faster, indicating lower amounts of lithium ions moving back to layer structure of cathode materials.

To examine the reactivity of NMC and NMC with Cu impurities, we conducted CV scans between 2.5 and 4.8 V (Figure 6). The scan rate was 0.1 mV/s. From the peaks at 3.75 V, it can be clearly observed that as the Cu amount increases, the peak becomes sharper and narrower. This is because NMC with Cu impurities have smaller particle sizes and larger contact area with the electrolyte, so the reaction is more active. However, the peak area becomes smaller as the Cu amount increases, agreeing with the lower specific discharge capacity result of NMC with Cu impurity. Another noticeable difference between these three CV curves is that, at around 4.6 V, there is a significant peak in the pure NMC scan result. But the peak is not as identifiable in NMC with 2.5 and 5 atom % Cu. It has been previously reported that Mn element is responsible for this peak.[18] In the NMC cathode materials with higher amounts of Cu impurities, this peak is very weak and almost disappears. This result supports the argument that in NMC with Cu impurity, the Cu occupies some Mn sites or inhibits the electrochemical reaction of Mn element.

4. CONCLUSION

NMC cathode materials with and without coper impurities were synthesized via a coprecipitation and solid state synthesis process. Crystal structure changes of NMC and NMC with impurities after electrochemical test were analyzed and discussed. The lattice parameters of synthesized pure NMC have a more significant change of c values, corresponding to the lower capacity retention. NMC cathodes with Cu impurities have a better capacity retention and smaller c value variation. Although the exact locations/activities of copper in the crystal structure is still not 100% clear, CV scan provide some evidence of Cu element reacting with Mn or occupying Mn sites in the NMC crystal structure. The initial capacity of material containing copper is slightly lower because of defect caused

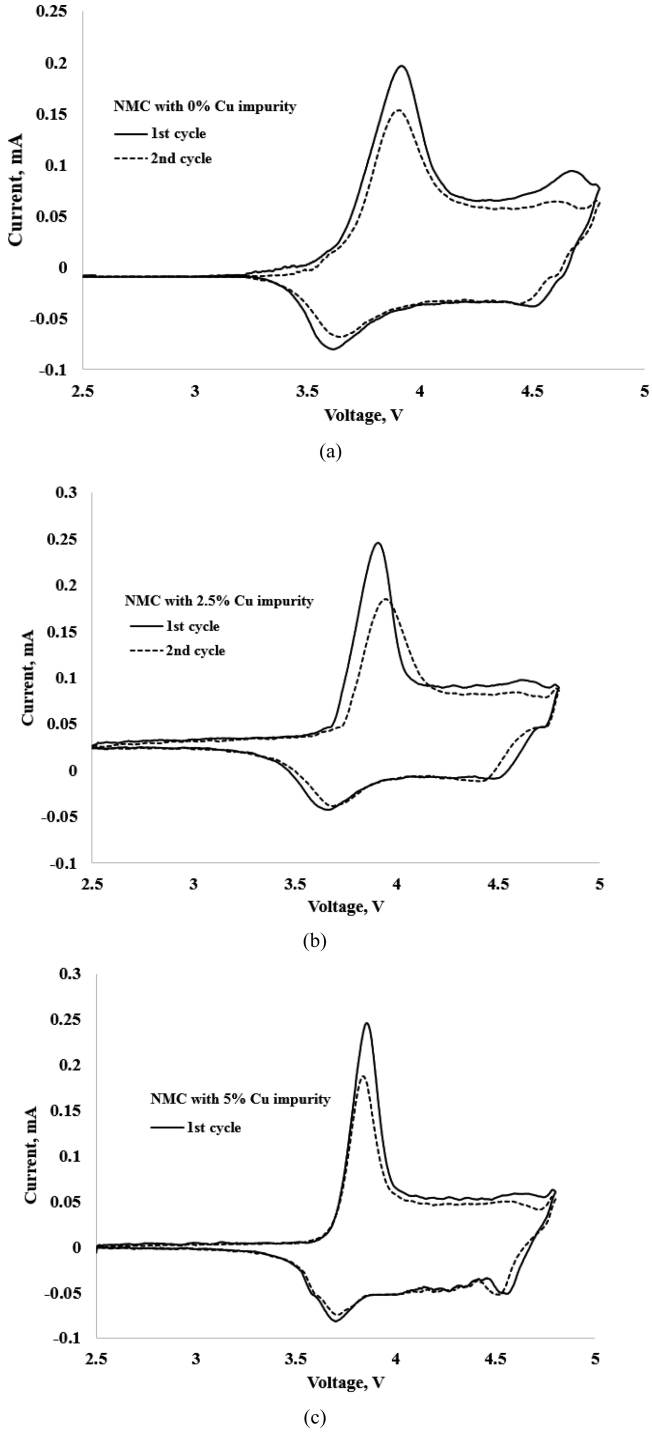

Figure 6. CV scan results of NMC with different amount copper impurity.

by the Cu impurity. However, it was revealed that the existence of a small atomic percent of copper helps stabilize the capacity retention. Future work will include Cu element activities in NMC crystal structure during charge−discharge process. In addition, the Cu effect to NMC cathode charges and discharges process at higher C rates or wider voltage ranges will be investigated.

DOI: 10.1021/acsami.5b04426
ACS Appl. Mater. Interfaces 2015, 7, 20585−20590

AUTHOR INFORMATION

Corresponding Author

* Tel.: 508-831-5453. Fax: 508-831-5178. E-mail: yanwang@wpi.edu.

Notes

The authors declare no competing financial interest.

ACKNOWLEDGMENTS

This work was financially supported by National Science Foundation (NSF) under grants 1230675 and 1343439 and 1464535. We acknowledge the helpful discussions with Prof. Emmert and Dr. Bandara who are colleagues at WPI's Center for Resource Recovery and Recycling (CR3 an NSF I/UCRC).

REFERENCES

(1) Richa, K.; Babbitt, C. W.; Gaustad, G.; Wang, X. A Future Perspective on Lithium-ion Battery Waste Flows from Electric Vehicles. *Resour. Conserv. & Recy.* **2014**, *83*, 63−76.

(2) Lee, C. K.; Rhee, K.-I. Preparation of $LiCoO_2$ from Spent Lithium-ion Batteries. *J. Power Sources* **2002**, *109*, 17−21.

(3) Shin, S. M.; Kim, N. H.; Sohn, J. S.; Yang, D. H.; Kim, Y. H. Development of a Metal Recovery Process from Li-ion Battery Wastes. *Hydrometallurgy* **2005**, *79*, 172−181.

(4) Li, J.; Shi, P.; Wang, Z.; Chen, Y.; Chang, C.-C. A Combined Recovery Process of Metals in Spent Lithium-ion Batteries. *Chemosphere* **2009**, *77*, 1132−1136.

(5) Wang, R.-C.; Lin, Y.-C.; Wu, S.-H. A Novel Recovery Process of Metal Values from the Cathode Active Materials of the Lithium-ion Secondary Batteries. *Hydrometallurgy* **2009**, *99*, 194−201.

(6) Lupi, C.; Pasquali, M.; Dell'Era, A. Nickel and Cobalt Recycling from Lithium-ion Batteries by Electrochemical Processes. *Waste Manage.* **2005**, *25*, 215−220.

(7) Zou, H.; Gratz, E.; Apelian, D.; Wang, Y. A Novel Method to Recycle Mixed Cathode Materials for Lithium Ion Batteries. *Green Chem.* **2013**, *15*, 1183−1191.

(8) Gratz, E.; Sa, Q.; Apelian, D.; Wang, Y. A Closed Loop Process for Recycling Spent Lithium Ion Batteries. *J. Power Sources* **2014**, *262*, 255−262.

(9) Sa, Q.; Gratz, E.; He, M.; Lu, W.; Apelian, D.; Wang, Y. Synthesis of High Performance $LiNi_{1/3}Mn_{1/3}Co_{1/3}O_2$ from Lithium Ion Battery Recovery Stream. *J. Power Sources* **2015**, *282*, 140−145.

(10) Liu, D.; Wang, Z.; Chen, L. Comparison of Structure and Electrochemistry of Al- and Fe- Doped $LiNi_{1/3}Mn_{1/3}Co_{1/3}O_2$. *Electrochim. Acta* **2006**, *51*, 4199−4203.

(11) Ding, Y.; Zhang, P.; Jiang, Y.; Gao, D. Effect of Rare Earth Elements Doping on Structure and Electrochemical Properties of $Li[Ni_{1/3}Mn_{1/3}Co_{1/3}]O_2$ for Lithium-ion Battery. *Solid State Ionics* **2007**, *178*, 967−971.

(12) Ye, S.; Xia, Y.; Zhang, P.; Qiao, Z.; Al, B.; Doped, F. $LiNi_{1/3}Mn_{1/3}Co_{1/3}O_2$ as Cathode Material of Lithium-ion Batteries. *J. Solid State Electrochem.* **2007**, *11*, 805−810.

(13) Lee, M. H.; Kang, Y. J.; Myung, S. T.; Sun, Y. K. Synthetic Optimization of $Li[Ni_{1/3}Mn_{1/3}Co_{1/3}]O_2$ via Co-precipitation. *Electrochim. Acta* **2004**, *50*, 939−948.

(14) Kim, G.-H.; Myung, S.-T.; Kim, H. S.; Sun, Y.-K. Synthesis of Spherical $Li[Ni_{(1/3-z)}Co_{(1/3-z)}Mn_{(1/3-z)}Mg_z]O_2$ as Positive Electrode Material for Lithium-ion Battery. *Electrochim. Acta* **2006**, *51*, 2447−2453.

(15) Lim, J.-H.; Bang, H.; Lee, K.-S.; Amine, K.; Sun, Y.-K. Electrochemical Characterization of Li_2MnO_3-$Li[Ni_{1/3}Co_{1/3}Mn_{1/3}]O_2$-$LiNiO_2$ Cathode Synthesized via Co-precipitation for Lithium Secondary Batteries. *J. Power Sources* **2009**, *189*, 571−575.

(16) van Bommel, A.; Dahn, J. R. Synthesis of Spherical and Dense Particles of the Pure Hydroxide Phase $Ni_{1/3}Mn_{1/3}Co_{1/3}(OH)_2$ Batteries and Energy Storage. *J. Electrochem. Soc.* **2009**, *156*, A362−A365.

(17) Li, D.-C.; Muta, T.; Zhang, L.-Q.; Yoshio, M.; Noguchi, H. Effect of Synthesis Method on the Electrochemical Performance of $LiNi_{1/3}Mn_{1/3}Co_{1/3}O_2$. *J. Power Sources* **2004**, *132*, 150−155.

(18) Choi, J.; Manthiram, A. Investigation of the Irreversible Capacity Loss in the Layered $LiNi_{1/3}Mn_{1/3}Co_{1/3}O_2$ cathodes. *Electrochem. Solid-State Lett.* **2005**, *8*, C102−C105.

(19) Rao, C. V.; Reddy, A.; L, M.; Ishikawa, Y.; Ajayan, P. $LiNi_{1/3}Co_{1/3}Mn_{1/3}O_2$−Graphite Composite as a Promising Cathode for Lithium-ion Batteries. *ACS Appl. Mater. Interfaces* **2011**, *3*, 2966−2972.

(20) Petersburg, C. F.; Li, Z.; Chernova, N. A.; Whittingham, M. S.; Alamgir, F. M. Oxygen and Transition Metal Involvement in the Charge Compensation Mechanism of $LiNi_{1/3}Mn_{1/3}Co_{1/3}O_2$ Cathodes. *J. Mater. Chem.* **2012**, *22*, 19993−20000.

(21) *Lange's Handbook of Chemistry*; Dean, J. A., Ed.; McGraw-Hill, Inc.: New York, 1992.

(22) van Bommel, A.; Dahn, J. R. Analysis of the Growth Mechanism of Coprecipitated Spherical and Dense Nickel, Manganese, and Cobalt-Containing Hydroxides in the Presence of Aqueous Ammonia. *Chem. Mater.* **2009**, *21*, 1500−1503.

(23) Shaju, K. M.; Subba Rao, G. V.; Chowdari, B. V. R Performance of layered $Li(Ni_{1/3}Co_{1/3}Mn_{1/3})O_2$ as cathode for Li-ion batteries. *Electrochim. Acta* **2002**, *48*, 145−151.

DOI: 10.1021/acsami.5b04426
ACS Appl. Mater. Interfaces 2015, 7, 20585−20590